Available online at www.sciencedirect.com
SCIENCE DIRECT
Polymer 46 (2005) 10758–10771
polymer
www.elsevier.com/locate/polymer

Reaction induced phase separation in semicrystalline thermoplastic/epoxy resin blends

G. Vanden Poel, S. Goossens, B. Goderis, G. Groeninckx*

Division of Polymer Chemistry, Laboratory of Macromolecular Structural Chemistry, Department of Chemistry, Catholic University of Leuven, Celestijnenlaan, 200F-3001 Heverlee, Belgium

Received 16 December 2004; received in revised form 14 July 2005; accepted 2 September 2005
Available online 28 September 2005

Abstract

The phase separation behaviour and phase morphology of blends of 4,4′-diaminodiphenyl sulphone cured diglycidyl ether of bisphenol-A with poly(ε-caprolactone) were investigated by means of scanning electron microscopy, small angle light scattering and optical microscopy. The components are miscible prior to curing. High-temperature isothermal curing induces phase separation. Blends with near to critical concentrations demix via spinodal decomposition. The associated co-continuous morphology is only preserved in the actual critical compositions whereas for off-critical compositions it rapidly breaks up into spherical particles. The proceeding reaction in the separated phases induces a secondary phase separation. Occasionally, tertiary phase separation is observed as well. Off-critical compositions that are further away on either side from the critical point, phase separate via the direct formation of spherical particles, most likely as a result of the dynamic asymmetry of these blends. The influence of the amount, the molar mass of PCL and the cure temperature is discussed.

Keywords: Epoxy/PCL blends; Reaction induced phase separation; Mechanism of phase separation

1. Introduction

Thermosetting polymers are used increasingly in engineering applications. They are amorphous, highly crosslinked polymers with excellent properties such as high tensile strength and modulus of elasticity, good thermal and chemical resistance, and dimensional stability. However, they suffer from low toughness and poor crack resistance, and they are normally brittle at room temperature. Therefore, thermosetting polymers are toughened for many end-use applications. One of the most successful methods consists of incorporating dispersed rubbery particles into the crosslinked polymer. The presence of a rubber phase increases the fracture resistance but decreases the elasticity modulus, yield strength and thermal stability of the material. Alternatively, thermoplastics can be introduced as dispersed phase. A two-phase morphology can be achieved by mechanically dispersing thermoplastic particles into the epoxy matrix or through phase separation driven by the curing reaction [1–4].

Most of the thermoplastic/thermosetting polymer blends start as a homogeneous liquid resin/thermoplastic polymer mixture but transform into a phase-separated structure due to the increasing molar mass or network formation of the thermoset [5,6]. The blend composition and the curing temperature determine the mechanism of reaction-induced phase separation, i.e. nucleation and growth or spinodal demixing [1–5,7–19], which in turn determines the morphology and thus the mechanical properties of the product. The composition of the initial blend in particular seems to be crucial [8–10]. Compositions close to the critical concentration separate via spinodal demixing, which yields a bi-continuous morphology [10]. For off-critical compositions, the second phase appears through nucleation and growth. In this case the thermoset component forms either the dispersed or the continuous phase depending on whether the thermoset concentrations is far above (supercritical concentrations) or far below the critical composition (subcritical concentrations).

Relatively few systematic studies dealt with the miscibility, phase behaviour and crystallisation in blends of thermosetting resins with crystallisable thermoplastic polymers. In such blends crystallisation is complicated as it is greatly affected by the blend miscibility and phase behaviour [20–23]. The interest in semicrystalline components is relevant as their introduction leads to an improved elastic modulus and heat resistance.

* Corresponding author. Tel.: +32 16 327440; fax: +32 16 327990.
E-mail address: gabriel.groeninckx@chem.kuleuven.ac.be (G. Groeninckx).

0032-3861/$ - see front matter © 2005 Elsevier Ltd. All rights reserved.
doi:10.1016/j.polymer.2005.09.013

In this research a model system, DGEBA/DDS/poly(ε-caprolactone), has been considered. Such blends can be prepared with a minimal mixing time and at sufficiently low temperatures to avoid curing reaction during mixing. The epoxy-oligomers and poly(ε-caprolactone), PCL, the thermoplastic semicrystalline component are miscible over the whole composition range, which is crucial in such work [23]. Reaction-induced phase separation (RIPS) only occurs at elevated temperatures above the melting point of PCL. In this paper, focus is on the influence of the cure temperature, the amount and the molecular mass of PCL on the morphology, phase separation mechanism and kinetics. The crystallisation behaviour and the semicrystalline morphology of PCL in DDS-cured epoxy/PCL blends will be discussed in a separate paper.

2. Experimental

2.1. Materials

The epoxy resin used here was a low molar mass liquid diglycidyl ether of bisphenol A (DGEBA) (Epikote 828LVEL, EEM 182–187 g, ICI, Belgium) with an epoxide equivalent weight of 5.36 mol/kg. The hardener used was 4,4′-diamino diphenyl sulphone (DDS) (Aldrich, $\bar{M}_w = 284$ g/mol, A7 480-7). The selected thermoplastics used in this study were commercial grade polycaprolactones (PCL): a low molar mass PCL (purchased from Janssen Chemical Company, Ltd, Belgium) with $\bar{M}_w = 5000$ g/mol, $T_g = -66.5$ °C and $T_m = 57.2$ °C, and a high molar mass PCL (purchased from Solvay Interox, Ltd, Great Britain, UK) with $\bar{M}_w = 50,000$ g/mol and $T_g = -65.7$ °C, $T_m = 57.3$ °C. The chemical structures of DGEBA, PCL and DDS are shown in Fig. 1.

2.2. Sample preparation

2.2.1. Mixtures with low molar mass PCL (5000 g/mol)

The PCL modified mixtures were prepared in a two-step process. PCL in various proportions was first dissolved in the epoxy prepolymer (DGEBA) by continuous stirring at 120 °C. The curing agent DDS was then added to the mixture under continuous stirring at 150, 180 and 200 °C, respectively, for approximately 15 s, and then immediately quenched in liquid nitrogen. A homogeneous ternary mixture was obtained. The extent of reaction after this preparation raised between 0.5 and 3%, as controlled by FT-IR measurements [24], depending on the samples. DDS was used at a stoichiometric ratio epoxy to amino-hydrogen groups equal to 1.

2.2.2. Mixtures with high molar mass PCL (50,000 g/mol)

The PCL was first dissolved in tetrahydrofuran (THF) at room temperature, afterwards the epoxy resin, DGEBA, was added and dissolved under continuous stirring. Next, the curing agent DDS was poured into the mixture and dissolved under the same conditions. After complete dissolution the solvent was removed from the homogeneous mixture by evaporating THF under vacuum during 12 h. Since there is no heating involved, it is assumed therefore that no curing reaction has occurred, and that it is thus possible to measure the epoxy-amine reaction from the very beginning at high temperatures. All the mixtures were prepared for future use and kept in a refrigerator at very low temperatures.

2.3. Techniques

2.3.1. Differential scanning calorimetry

Dry nitrogen gas was purged to provide the Perkin Elmer Pyris 1 DSC with an inert environment. Indium and benzophenone standards were used for temperature and enthalpy calibration. The sample mass was between 5 and 10 mg.

For the study of the initial component miscibility, all samples were first heated and kept for 5 min at 100 °C to destroy their thermal history without inducing any curing reaction; subsequently they were cooled at a rate of 10 °C/min to a temperature of −70 °C where they were kept for another 5 min. Finally a heating scan at a rate of 10 °C/min was conducted to measure the glass transition temperature (T_g) of the blend systems. In systems where PCL was able to crystallise during cooling, quenched samples were used to obtain the T_g value, in order to minimise crystallisation induced segregation that would alter the amorphous fraction composition and hence the T_g. The crystallisation temperature (T_c) corresponds to the minimum of the exothermic peak and the melting temperature (T_m) to the maximum of the endothermic peak.

2.3.2. Scanning electron microscopy

Morphological investigations were performed with a scanning electron microscopy (SEM) (model XL20, Philips Co.). The samples after curing at 150, 180 and 200 °C for 4 h, were fractured in liquid nitrogen. The broken surfaces were

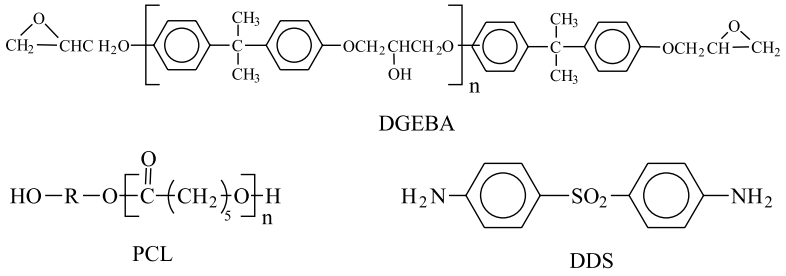

Fig. 1. Chemical structure of DGEBA, PCL and DDS.

etched with chloroform in order to remove the thermoplastic component, and dried over night under vacuum to remove the last traces of the solvent. Each specimen was then sputter coated with a thin layer of gold to improve the electron conductivity before taking the SEM micrographs.

The average PCL rich particle size and size distribution were calculated for blends with an epoxy-rich matrix using (manually) binarised micrographs and a script within the image analysis program Qwin of Leica. The number average diameter, $\overline{D_n}$, the volume average diameter, $\overline{D_v}$, and the polydispersity, P, were calculated according to

$$\overline{D_n} = \frac{\sum_i n_i d_i}{\sum_i n_i} \tag{1}$$

$$\overline{D_v} = \frac{\sum_i n_i d_i^4}{\sum_i n_i d_i^3} \tag{2}$$

$$P = \frac{\overline{D_v}}{\overline{D_n}} \tag{3}$$

were n_i is the number of particles with diameter d_i. N the average number of particles per unit volume was calculated from V, the particle volume fraction—taken to be equal to the observed particle 2D fraction—using

$$N = \frac{V}{\left[\frac{\pi}{6}\overline{D_n}^3\right]} \tag{4}$$

To obtain a good statistical distribution, more than 500 particles for one particular blend composition were investigated. The described procedure could not be used to characterise epoxy rich particles because binarisation in this case was impossible.

2.3.3. Small angle laser light scattering (SALLS)

A SALLS set-up was used similar to the one described by Ishii and Ryan [11]. It consists of a polarized 1 mW Spectra-Physics 117A type He/Ne laser ($\lambda = 632.8$ nm), a polarizer set parallel to the polarization of the laser, the sample in a Mettler FP82-HT hot stage, a second polarizer (analyzer) oriented with its polarization parallel (Vv SALLS) to that of the first one, a screen with a beam catcher on which the scattering patterns are projected and a Photometrix ATC200L cooled CCD detector. The scattering angles are calibrated with a 100 lines/mm grid. Samples, sandwiched between two glass slides, are inserted into the hot stage. Scattered intensities were measured during isothermal curing every 15 s. The data acquisition time is typically 10 ms and was controlled by a PC based integrated home-made script running under V for Windows (version 3.5b, Digital Optics Ltd). This software also takes care of some on line image processing, such as the integration of the scattered intensities, resulting in the relative total light scattering intensity and an azimuthal averaging of the 2D patterns. The scattering angle, θ, is expressed as $q = (4\pi/\lambda)\sin(\theta/2)$, the modulus of the scattering vector.

2.3.4. Optical microscope

Direct space information on the phase separation and the overall morphology was obtained by an Olympus BH_2 optical microscope (OM). The samples were placed between two glass cover slips and the temperature was controlled by a Mettler FP82-HT hot stage. Digital micrographs were taken at different cure times by a JVC TK-C1381 CCD camera, controlled by the program Qwin of the Leica Company.

2.3.5. Dynamic mechanical analysis

Sheets were obtained by putting the mixtures into a silicone mould with suitable dimensions for dynamic mechanical analysis (DMA). Blends with a PCL molecular mass of 5000 g/mol were cured in an oven at 150, 180 or 200 °C for different curing times. After a given cure time the samples were quenched into liquid nitrogen by which the reaction stops. Next, the visco-elastic properties of the DDS-cured DGEBA/PCL blends were measured using a TA instruments DMA 2980, applying the three point bending mode at a frequency of 10 Hz between room temperature and 250 °C at a heating rate of 3 °C/min. Only the glass transition of the epoxy rich phase, T_g, appears above room temperature and was identified at the maximum of the tan δ. This T_g increases with curing time and at a given time it reaches the curing temperature. This time is reported.

3. Results

3.1. Miscibility of uncured DGEBA/PCL blends

Miscibility can be asserted by evaluation of the glass transition behaviour using DSC. Fig. 2(a) and (b) show the DSC thermograms of the uncured DGEBA/$PCL_{50,000}$ and DGEBA/PCL_{5000} blends, respectively. Well-defined, single glass transition temperatures (T_g) are observed in both figures over the whole composition range, indicating that both uncured systems are completely miscible. The results are summarised in Fig. 3(a) and (b), illustrating that the experimental T_g data can be very well fitted by the Gordon–Taylor equation [25] (straight line through full circles).

$$T_g(\text{Blend}) = \frac{\omega(\text{PCL}) \times T_g(\text{PCL}) + k\omega(\text{DGEBA}) \times T_g(\text{DGEBA})}{\omega(\text{PCL}) + k\omega(\text{DGEBA})}$$

where T_g (Blend) is the glass transition temperature of the blend; T_g (DGEBA) and T_g (PCL) are the T_g's of DGEBA and PCL, respectively; ω (DGEBA) and ω (PCL) represent the weight fractions of DGEBA and PCL, respectively; k is a constant. The fitting curves (full lines) in Fig. 3(a) and (b) are drawn using k values of 1.10 and 1.03, respectively. The peaks in the thermograms related to the PCL crystallisation and melting are added to Fig. 3 for completeness but will further not be discussed.

3.2. Onset of phase separation

The onset of phase separation for all DDS-cured DGEBA/PCL blends was identified by SALLS as the first

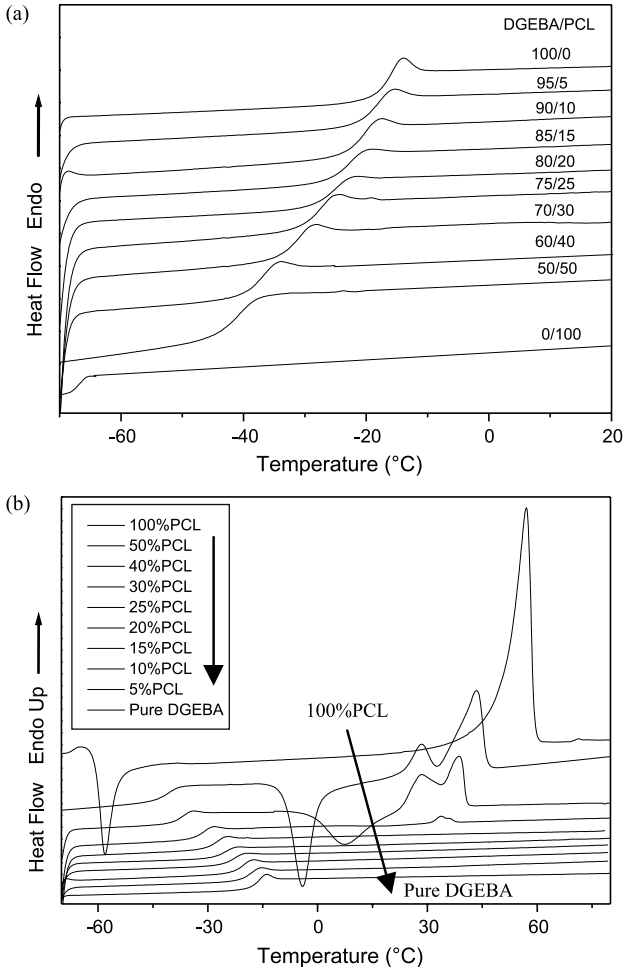

Fig. 2. DSC curves of samples prior to curing: (a) DGEBA/$PCL_{50,000}$ and (b) DGEBA/PCL_{5000} blends (heating rate 10 °C/min).

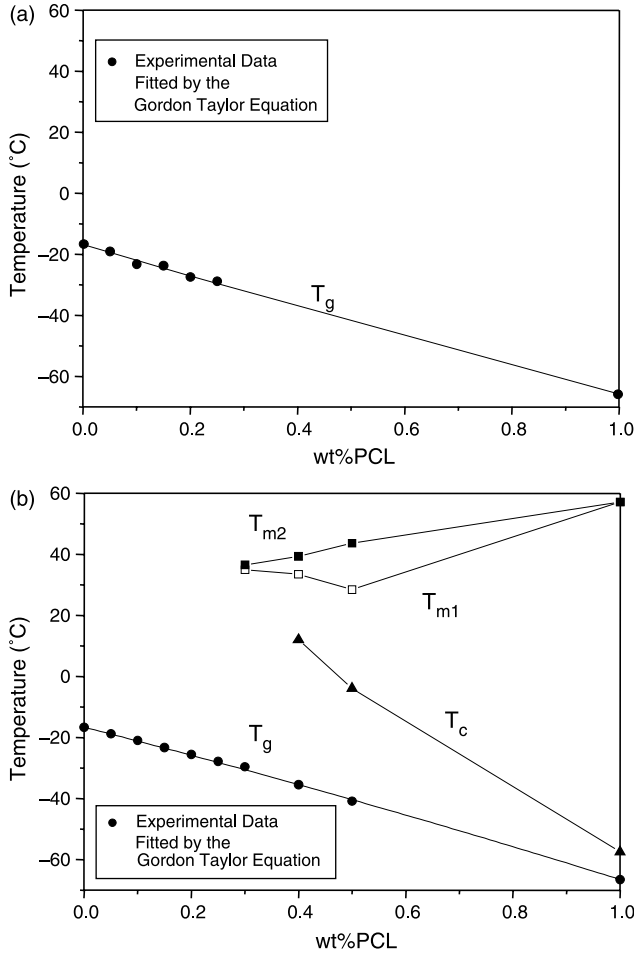

Fig. 3. Thermal transitions in the samples prior to curing: (a) DGEBA/$PCL_{50,000}$ and (b) DGEBA/PCL_{5000} blends.

increase of the scattered intensity above the background signal. The associated cure times for the different blend compositions at different cure temperatures (150, 180 and 200 °C), are summarised in Fig. 4(a) and (b). Clearly, phase separation starts earlier with increasing cure temperature and with increasing PCL molar mass. The latter effect can be better observed at lower cure temperature. Furthermore, the phase separation onset shifts to later times with increasing PCL wt%. At the low PCL wt% side the onset of phase separation should evolve towards infinite times (dashed lines in Fig. 4), as a neat epoxy resin will never phase separate.

3.3. Phase morphology by SEM

The morphologies of DDS-cured DGEBA/PCL_{5000} blends after 4 h curing at 150, 180 and 200 °C are represented in Fig. 5(A)–(C), respectively. Recall that only the epoxy-rich phase is visible in these micrographs as the PCL rich phase is selectively dissolved in the treatment. The blends containing 20 wt% PCL_{5000} or less, exhibit a particle/matrix morphology where the (removed) PCL_{5000}-rich phase is dispersed in an epoxy-rich matrix. The particle sizes of these dispersions are listed in Table 1. At a given cure temperature, the average particle diameter ($\bar{D}_n, \bar{D}_v$) increases with increasing PCL_{5000} concentration and also increases with increasing cure temperature at constant PCL_{5000} concentration. Table 2 furthermore reveals an increase of V and a decrease of N with increasing cure temperature or amount of PCL_{5000}. In all cases, V, is larger than the initial PCL (mass) fraction and this relative excess increases with increasing cure temperature. This points to an increasing degree of partial miscibility between the epoxy resin components with PCL_{5000}.

Blends containing 30 wt% PCL_{5000} and more, exhibit a phase-inverted structure where the closely stacked and interconnected epoxy beads are imbedded in a continuous PCL-rich matrix (Fig. 5(A)–(C)). Even without performing any statistical analysis it is clear that the bead size decreases and the bead size distribution gets narrower with increasing amount of PCL. This holds for all cure temperatures. Fig. 6 shows fractured epoxy beads for the sample with 30 wt% PCL_{5000}, indicating the existence of etchable PCL rich sub-inclusions. This points at a double phase separation.

In the composition range between 20 and 30 wt% PCL_{5000} a co-continuous morphology with strongly interpenetrating phase domains is observed of which the two phases each resemble the structure that is observed at respectively lower (PCL rich droplets in an epoxy-rich matrix) and higher

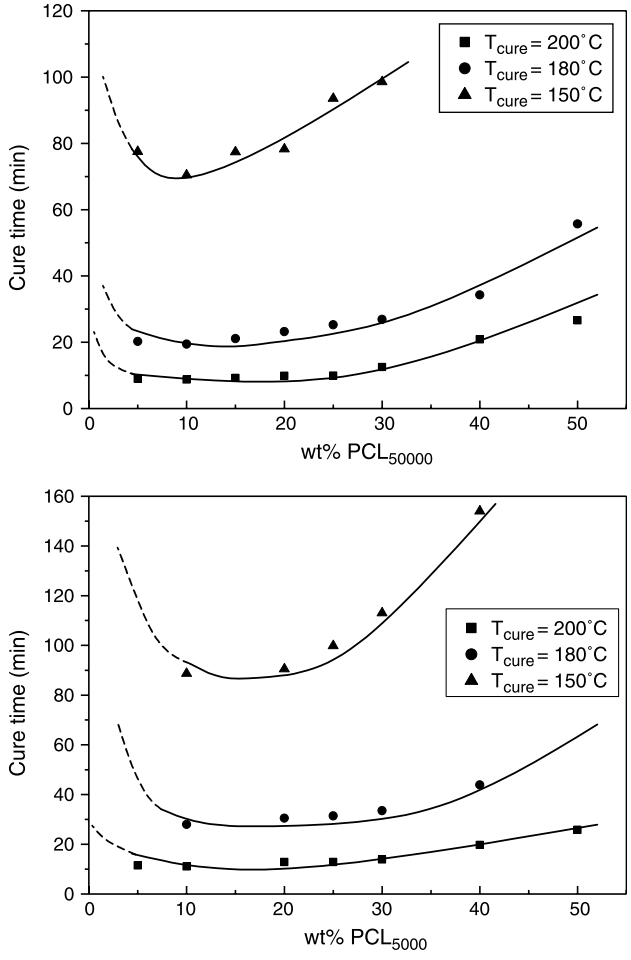

Fig. 4. Onset of phase separation for (a) DGEBA/$PCL_{50,000}$ and (b) DGEBA/PCL_{5000} blends at different isothermal cure temperatures (T_{cure}).

(epoxy beads with PCL-rich sub-inclusions in a PCL rich matrix) PCL_{5000} wt% (Fig. 5(Ac), (Bc), (Cc)). Fig. 5(Bc) in particular is interesting as it was taken at a lower magnification. This morphology again points at phase separation in—at least—two steps as will be discussed in the appropriate section below. The term 'at least' refers at the presence of small etchable PCL rich sub-inclusions inside the larger epoxy beads, which is a signature of tertiary phase separation in this case.

Similar observations were made in blends containing PCL with a higher molar mass (50,000 g/mol). Compositions up to 10 wt% $PCL_{50,000}$ give rise to a particle/matrix morphology and blends containing 20 wt% $PCL_{50,000}$ or more exhibit a phase inverted structure, except when the 20 wt% sample is cured at 150 °C for which a co-continuous structure is observed. The 15 wt% $PCL_{50,000}$ blend displays a co-continuous morphology irrespective of the curing temperature. Hence, the co-continuous domain occurs at a lower $PCL_{50,000}$ content than for the blends with PCL_{5000}. The increase of the particle size with increasing PCL concentration and curing temperature for the blends with a particle/matrix morphology is observed as well (Table 3). On the other hand, the trends in V and N observed earlier for the PCL_{5000} blends are not clear here (Table 4). The particle size of the phase inverted blends decreases with increasing amount of $PCL_{50,000}$.

The phase morphologies after 240 min of curing are summarised in the Tables 5 and 6 for PCL_{5000} and $PCL_{50,000}$, respectively. For the PCL_{5000} blends also the times at which the DMA based T_g crosses the curing temperature are indicated between brackets. With this approach it was only possible to catch the T_g for blends with a particle matrix or a co-continuous morphology since in phase-inverted structures it is essentially the (melted) PCL rich matrix that contributes to the DMA behaviour in the temperature range where the epoxy rich phase presumably has its T_g. This explains why T_g data for compositions above 25% PCL_{5000} are missing. The time to vitrify increases with increasing PCL wt%. Vitrification occurs earlier with increasing cure temperature for the 5 and 15 wt% PCL_{5000} samples, but passes a minimum time for the sample with 25 wt% PCL_{5000}. Vitrification always follows phase separation and occurs prior to the SEM morphological analysis for the 5 and 15 wt% PCL samples except for the 15 wt% sample cured at 150 °C. Vitrification does not occur prior to the SEM analysis for the 25 wt% sample.

3.4. Mechanism of phase separation

Fig. 7 displays snap shots of the OM based morphology during curing at 180 °C for the (a) 15 wt% PCL_{5000}, (b) 25 wt% PCL_{5000} and (c) 50 wt% PCL_{5000} blends. Blends with a lower PCL_{5000} concentration do not reveal any clear features in OM due to the small length scale involved: most of the PCL rich droplet diameters are below 1 μm (Fig. 5(Ba) and Table 1). In fact this also holds for the 15 wt% sample. However, in this particular case a slightly larger bi-continuous structure is seen at the onset of phase separation, which quite rapidly breaks up into spherical particles. The latter process is not finished yet in the image taken after 36 min. The final stage involving small droplets can better be observed with SEM and resembles the morphologies of the neighbouring compositions displayed in the Fig. 5(Aa) and (Ab). Clearly, the initial phase separation for the 15 wt% PCL_{5000} blend cured at 180 °C has spinodal characteristics. The evolution towards a particle/matrix morphology seems classical and to be associated with phase differentiation, a drift away from equal phase fractions and an increase of the interfacial tension. The final volume fraction occupied by the PCL_{5000} rich phase in this sample is 27% (Table 2).

Spinodal decomposition can clearly be observed for the 25 wt% PCL_{5000} blend on a larger length scale (Fig. 7 column b). The phases coarsen with time but do not drift far away from the 50% phase occupancy, indicating the proximity of a critical point [26]. Moreover the image taken after 82 min reveals a secondary phase separation, i.e. the development of small darker droplets inside the brighter phase (in this image). Comparison with the corresponding SEM micrograph identifies them as epoxy-rich droplets that develop in the initial PCL_{5000} rich phase. The PCL_{5000} droplets that—at least according to the SEM images—develop in the epoxy rich phase could not be seen by OM as they are too small. The observation of growing droplets is compatible with a secondary phase separation by a nucleation and growth process. However, droplets can also be formed in

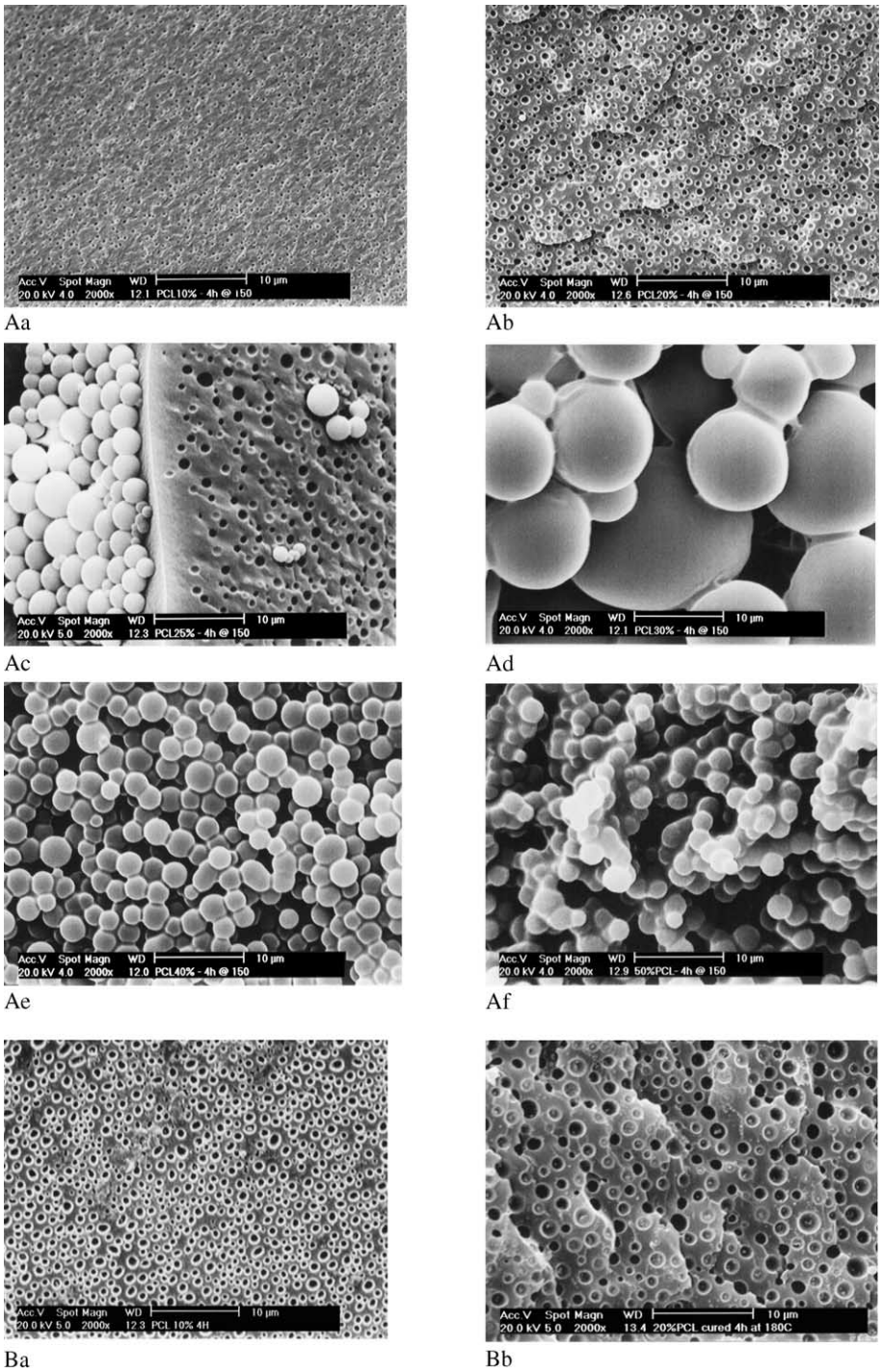

Fig. 5. (A) SEM micrographs of DGEBA/PCL_{5000} after 4 h curing at 150 °C: (Aa) 10 wt%, (Ab) 20 wt%, (Ac) 25 wt%, (Ad) 30 wt%, (Ae) 40 wt% and (Af) 50 wt% PCL_{5000}. (B) SEM micrographs of DGEBA/PCL_{5000} after 4 h curing at 180 °C: (Ba) 10 wt%, (Bb) 20 wt%, (Bc) 25 wt% (different magnification), (Bd) 30 wt%, (Be) 40 wt% and (Bf) 50 wt% PCL_{5000}. (C) SEM micrographs of DGEBA/PCL_{5000} after 4 h curing at 200 °C: (Ca)10 wt%, (Cb) 20 wt%, (Cc) 25 wt% and (Cd) 30 wt% PCL_{5000}.

the unstable region of the phase diagram, in particular for dynamically asymmetric mixtures [27]. This notion will be developed in Section 4. The presence of growing particles will nominally be associated with demixing via nucleation and growth throughout the result section.

In Fig. 7(c) multiple tiny, but growing droplets can be observed in the 50 wt% PCL_{5000} blend. As mentioned such a morphology development is compatible with liquid–liquid phase separation via a nucleation and growth mechanism.

For an assignment of the phase separation mechanism also the evolution of the SALLS patterns can be used. This approach is illustrated in Fig. 8(a)–(d) for the 10, 15, 25 and 30% $PCL_{50,000}$ blends, respectively, during curing at 180 °C. The SEM based morphologies after 4 h of curing are included as well.

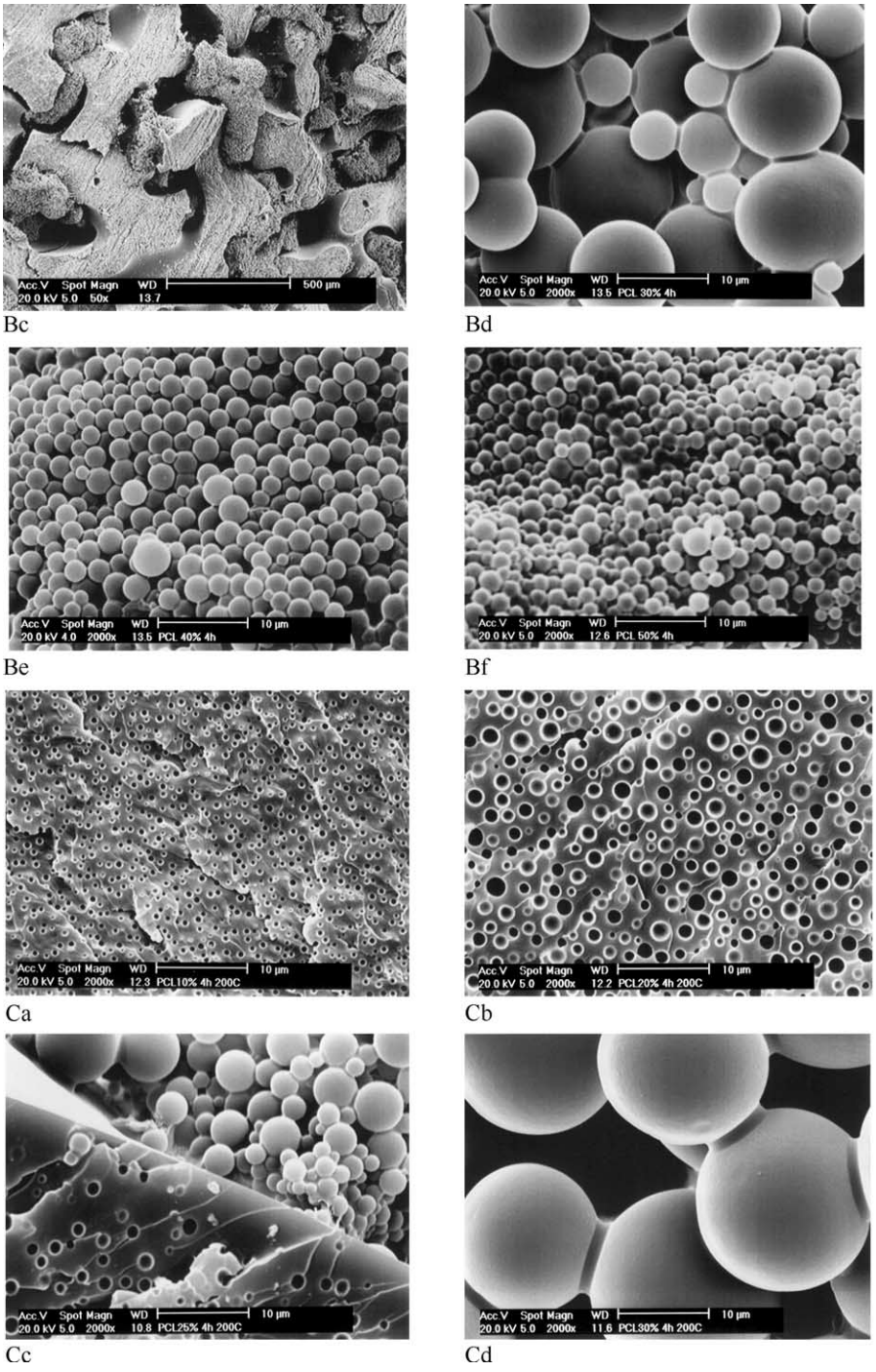

Fig. 5 (*continued*)

Table 1
Morphological parameters of the dispersed PCL-rich particles in DDS-cured DGEBA/PCL_{5000} blends

wt% PCL	$T_{cure}=150$ °C			$T_{cure}=180$ °C			$T_{cure}=200$ °C		
	$\bar{D}_n$ (µm)	$\bar{D}_v$ (µm)	P	$\bar{D}_n$ (µm)	$\bar{D}_v$ (µm)	P	$\bar{D}_n$ (µm)	$\bar{D}_v$ (µm)	P
10	0.36	0.42	1.19	0.56	0.61	1.07	0.63	0.68	1.08
15	0.43	0.48	1.13	0.75	0.85	1.13	0.85	0.95	1.12
20	0.67	0.83	1.24	1.28	1.54	1.20	1.44	1.70	1.19

Table 2
Final volume fraction of the dispersed phase, V, and number of particles per unit volume, N, as a function of the cure temperature in DDS-cured DGEBA/PCL_{5000} blends

T_{cure}	10 wt% PCL		15 wt% PCL		20 wt% PCL	
	V	N (μm^{-3})	V	N (μm^{-3})	V	N (μm^{-3})
150	0.11	4.50	0.19	4.65	0.28	1.78
180	0.14	1.52	0.27	1.22	0.33	1.17
200	0.19	1.45	0.28	0.87	0.34	0.22

The spherical particles generated in a nucleation and growth mechanism produce scattering that decays towards larger scattering angles according to the sphere form factor. The scattered intensity increases with increasing volume fraction of spheres, provided this fraction stays below 50% since the total scattering is proportional to the product $V(1-V)$. The intensities as a whole shift to smaller angles as the particle size increases during growth. A typical nucleation and growth decomposition is represented in Fig. 8(a). These scattering patterns are associate with the curing of a 10 wt% $PCL_{50,000}$ blend at 180 °C. The scattered intensity suddenly increases at the onset of phase separation and continues to do so during further curing up to about 30 min of curing. The sphere volume fraction after 4 h of curing is only 11.8% (Table 4) and hence did not cross the 50% border. The intensity decrease after about 30 min must thus be due to the growth of the particles and a shift of the scattering patterns towards smaller angles behind the beam stop. Alternatively, the refractive indices of the phases may approach while the curing reaction is going on. This reduction in contrast for scattering was termed 'apparent phase dissolution' by Inoue et al., [9]. In any case, the final morphology is a particle/matrix structure (see SEM micrograph in Fig. 8(a)). Comparable behaviour is observed for the 5 wt% $PCL_{50,000}$, 5 wt% PCL_{5000} and 10 wt% PCL_{5000} blends, irrespective of the cure temperature.

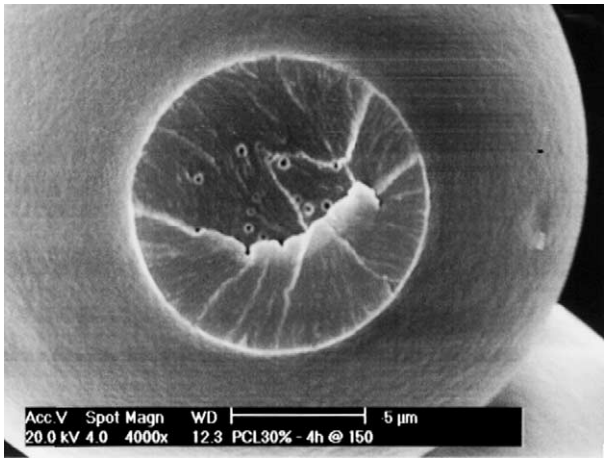

Fig. 6. SEM micrograph of an epoxy-rich particle fractured at an interglobular junction in a 30 wt% PCL_{5000} blend after 4 h curing at 150 °C.

Spinodal decomposition produces a peak in the SALLS patterns with a maximum at, q_{max}, which is associated with a characteristic length, l_C, given by $l_C=(2\pi)/q_{max}$. This characteristic length corresponds to the distance between similar phases, separated by the other phase and measured from centre to centre. In other words it corresponds to the structures' characteristic wavelength. In general three stages can be distinguished in a spinodal process. Theory predicts that in the early stage, while concentration fluctuations increase in amplitude, l_C stays constant [28]. In the intermediate stage l_C shifts towards smaller angels (larger distances) as the phase compositions further differentiate, the phase volume fractions drift away from the initial 50% and as the interfaces become increasingly sharp. Finally, in the late stage the interface sharpness and volume concentrations are fixed and only

Table 3
Morphological parameters of the dispersed PCL-rich particles in DDS-cured DGEBA/$PCL_{50,000}$ blends

wt% PCL	$T_{cure}=150$ °C			$T_{cure}=180$ °C			$T_{cure}=200$ °C		
	$\bar{D}_n$ (μm)	$\bar{D}_v$ (μm)	P	$\bar{D}_n$ (μm)	$\bar{D}_v$ (μm)	P	$\bar{D}_n$ (μm)	$\bar{D}_v$ (μm)	P
5	0.27	0.31	1.14	0.51	0.6	1.17	0.36	0.45	1.26
7.5	–	–	–	0.59	0.67	1.14	–	–	–
10	0.33	0.41	1.25	0.79	1.43	1.81	0.74	0.90	1.22

Table 4
Final volume fraction of the dispersed phase, V, and number of particles per unit volume, N, as a function of the cure temperature in DDS-cured DGEBA/$PCL_{50,000}$ blends

T_{cure}	5 wt% PCL		7.5 wt% PCL		10 wt% PCL	
	V	N (μm^{-3})	V	N (μm^{-3})	V	N (μm^{-3})
150	0.072	6.99	–	–	0.110	5.84
180	0.100	1.44	0.119	1.23	0.118	0.46
200	0.042	1.72	–	–	0.106	0.50

Table 5
Mechanism of phase separation (left) by SALLS and the SEM based morphology after 240 min of curing (right) as a function of the cure temperature and PCL contents in DDS-cured DGEBA/PCL_{5000} blends

wt% PCL_{5000}	Mechanism of phase separation			Phase morphology after 240 min		
	$T_{cure}=200$ °C	$T_{cure}=180$ °C	$T_{cure}=150$ °C	$T_{cure}=200$ °C	$T_{cure}=180$ °C	$T_{cure}=150$ °C
5	NG (11.5)	NG (28.5)	NG (90)	P/M (105)	P/M (143)	P/M (224)
10	NG (11.1)	NG (28.0)	NG (88.7)	P/M	P/M	P/M
15	(12)	SD* (29.0)	(89.5)	P/M (152)	P/M (158)	P/M (262)
20	SD (12.9)	SD (30.5)	SD (90.5)	P/M	P/M	P/M
25	SD (12.9)	SD (31.4)	SD (99.8)	Co–co (480)	Co–co (243)	Co–co (284)
30	SD (13.7)	SD (33.5)	SD (113.0)	Ph I	Ph I	Ph I
40	SD (19.8)	SD (43.9)	SD (154.0)	Ph I	Ph I	Ph I
50	NG (25.8)	NG*		Ph I	Ph I	Ph I

The numbers between brackets in the left part of the table are the onset times of phase separation. In the right hand side part the numbers indicate the time of vitrification for a selected number of samples. Data labeled with an asterisk are deduced via optical microscopy. In these cases SALLS did not give clear results.

Table 6
Mechanism of phase separation (left) by SALLS and the SEM based morphology after 240 min of curing (right) as a function of the cure temperature and PCL contents in DDS-cured DGEBA/$PCL_{50,000}$ blends

wt% $PCL_{50,000}$	Mechanism of phase separation			Phase morphology after 240 min		
	$T_{cure}=200$ °C	$T_{cure}=180$ °C	$T_{cure}=150$ °C	$T_{cure}=200$ °C	$T_{cure}=180$ °C	$T_{cure}=150$ °C
5	NG (9.0)	NG (20.3)	NG (77.5)	P/M	P/M	P/M
10	NG (8.7)	NG (19.4)	NG (70.4)	P/M	P/M	P/M
15	SD (9.2)	SD (21.1)	SD (77.4)	Co–co	Co–co	Co–co
20	SD (9.9)	SD (23.2)	SD (78.3)	Ph I	Ph I	Co–co
25	SD (9.9)	SD (25.3)	SD (93.5)	Ph I	Ph I	Ph I
30	NG (12.5)	NG (26.9)	NG (98.6)	Ph I	Ph I	Ph I
40	NG (20.9)	NG (34.3)		Ph I	Ph I	Ph I
50	NG (26.6)	NG (55.7)		Ph I	Ph I	Ph I

The numbers between brackets in the left part of the table are the onset times of phase separation.

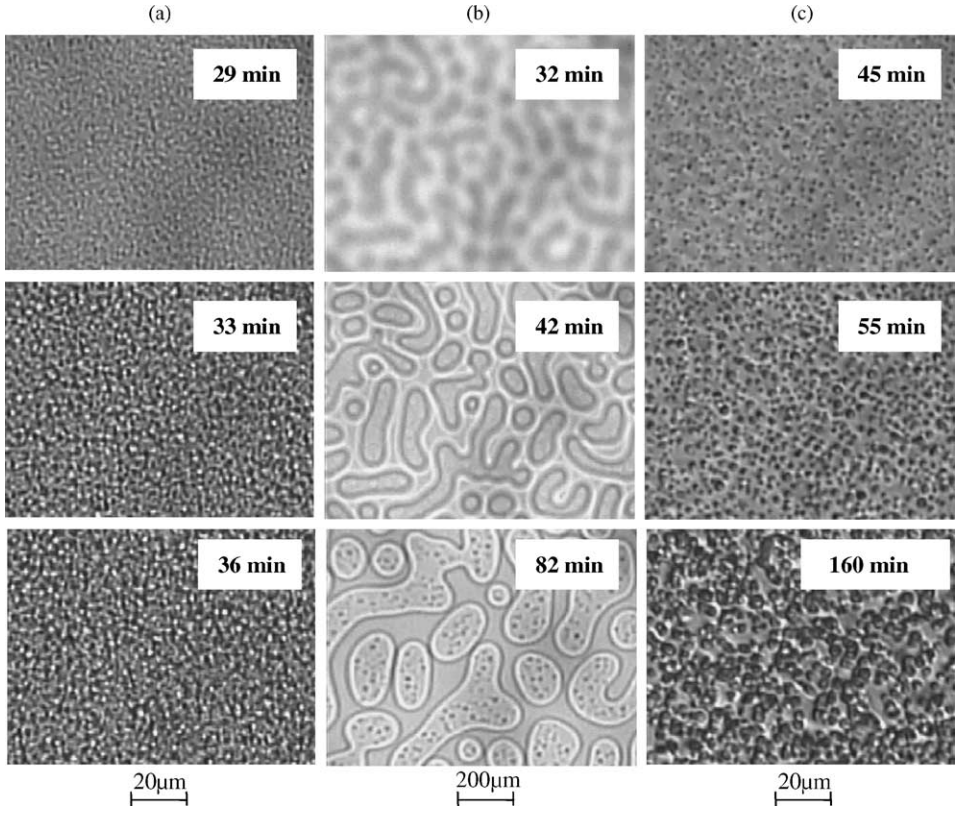

Fig. 7. Optical microscopy images captured during the curing at 180 °C at the indicated times. The first, second and third columns are associated with 15, 25 and 50 wt% PCL_{5000} blends, respectively. The first images (first row) were taken closely after the onset of phase separation.

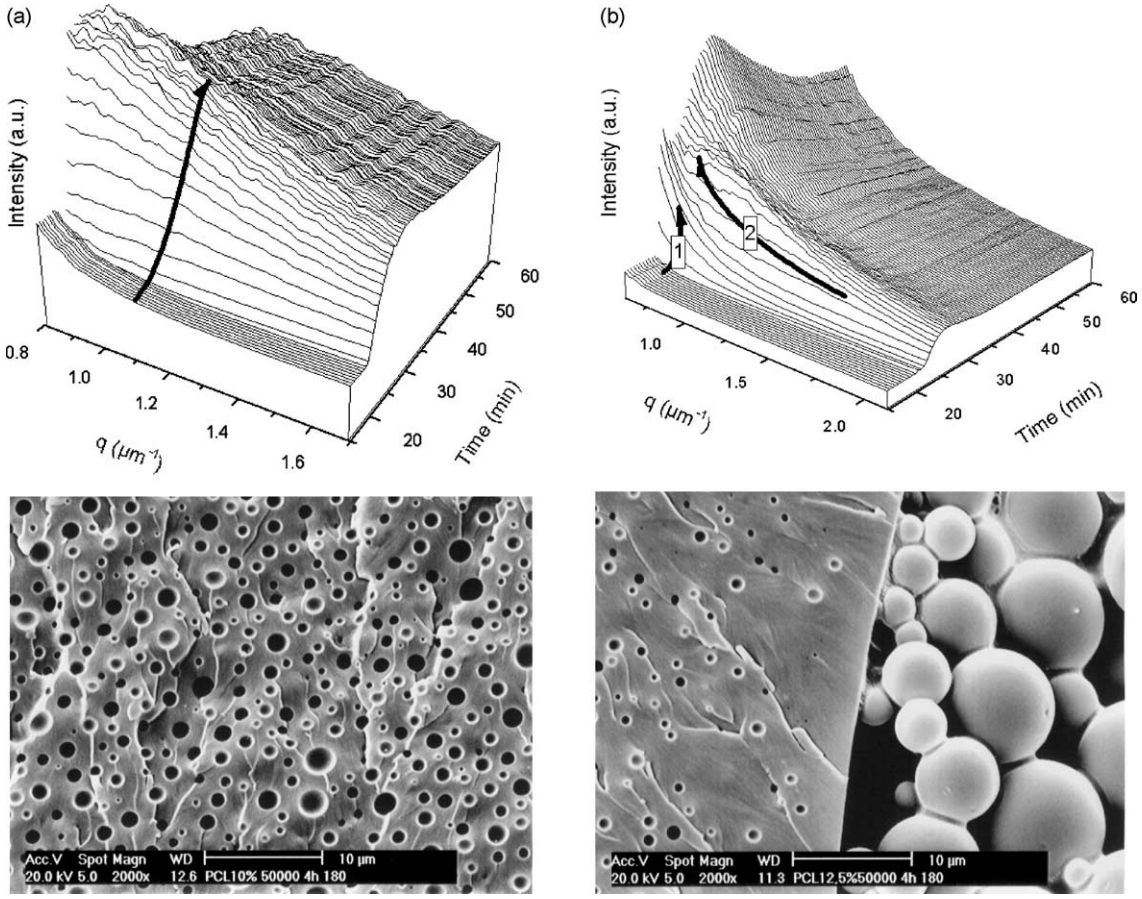

Fig. 8. (a) Time resolved evolution of the SALLS scattering patterns during the curing of a 10 wt% $PCL_{50,000}$ blend at 180 °C. The arrow is explained in the text. The corresponding SEM based morphology after 4 h curing is included below. (b) Time resolved evolution of the SALLS scattering patterns during the curing of a 15 wt% $PCL_{50,000}$ blend at 180 °C. The arrows are explained in the text. The corresponding SEM based morphology after 4 h curing is included below. (c) Time resolved evolution of the SALLS scattering patterns during the curing of a 25 wt% $PCL_{50,000}$ blend at 180 °C. The arrows are explained in the text. The corresponding SEM based morphology after 4 h curing is included below. (d) Time resolved evolution of the SALLS scattering patterns during the curing of a 30 wt% $PCL_{50,000}$ blend at 180 °C. The arrows are explained in the text. The corresponding SEM based morphology after 4 h curing is included below.

coarsening is left, driven by the tendency to reduce the amount of interfacial area.

In the present systems spinodal decomposition can occur at a length scale, which is in fact too large for SALLS, as, e.g. during the demixing of the 25 wt% PCL_{5000} blend discussed earlier and displayed in Fig. 7(b). The 15 wt% $PCL_{50,000}$ blends demixes in a comparable way at 180 °C and SALLS scattering patterns as in Fig. 8(b) are generated. At the onset of phase separation a strong increase in scattering is seen at the smallest angles (arrow 1). Here, q_{max} occurs behind the beam stop, preventing the characterisation of this spinodal structure. However, shortly after this first spinodal decomposition SALLS intensity appears at higher q-values with characteristics as observed earlier for the 10 wt% $PCL_{50,000}$ sample in Fig. 8(a) (see arrow 2 in Fig. 8(b)). Accordingly, spherical particles develop in a second stage. The observed part of the scattering patterns after 60 min of curing are compatible with particles of about 10 μm in diameter. The accompanying SEM picture reveals a given particle size distribution, but indeed spheres with such dimensions are also present. SALLS is particularly sensitive to the largest particles. Such a sequence of scattering patterns is observed for the 25 wt% PCL_{5000} and 15 wt% $PCL_{50,000}$ blends, irrespective of the curing temperature and for the 20 wt% $PCL_{50,000}$ blend cured at 150 °C.

At the other extreme l_C can be rather small for SALLS. Examples of that kind can only be found in the PCL_{5000} blend series, i.e. the 15 wt% and the 20 wt% sample with l_C values close to 2 μm and thus q_{max} values close to 3 μm^{-1}, the limit of the SALLS setup used at the time of the measurements. The scattering patterns are rather flat and display only a faint maximum at the onset of phase separation. Moreover, it disappears quite rapidly. Such a behaviour is expected from what the OM images show for the 15 wt% PCL_{5000} sample in Fig. 7(a): a spinodal structure that breaks up into particles in the intermediate stage.

Occasionally, l_C, appears in the experimental SALLS window as illustrated in Fig. 8(c) for the 25 wt% $PCL_{50,000}$ blend during curing at 180 °C. Typical early stage behaviour is missing, since the maximum associated with l_C shifts to smaller angles immediately after the phase separation onset (arrow 1 in Fig. 8(c)) and finally also disappears partially behind the beam stop. Shortly after, a shoulder appears on the high angle wing of the spinodal scattering pattern with a shape characteristic of spherical particles with a diameter of about 10 μm (arrow 2).

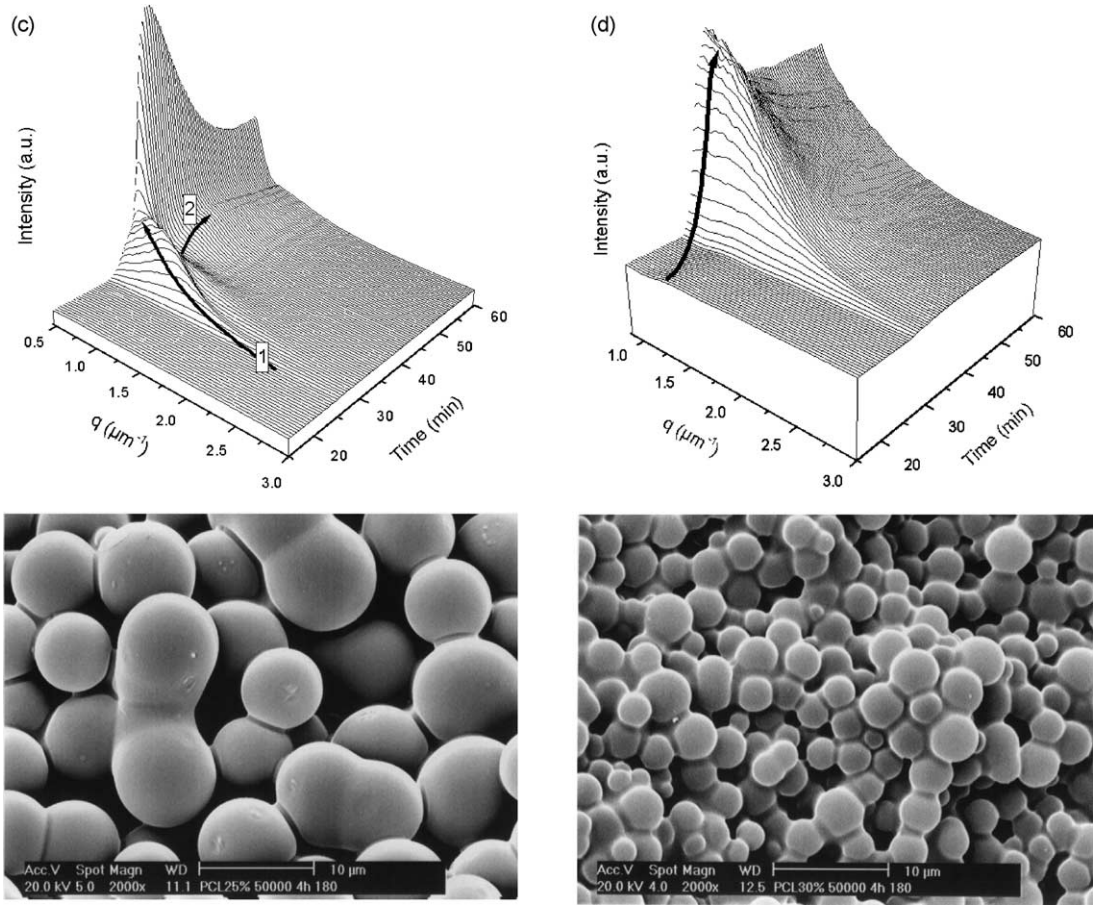

Fig. 8 (*continued*)

These spheres are not generated by the growth of small nuclei because no scattering is observed at higher angles prior to the appearance of the shoulder. Accordingly, these spheres are most likely the result of a break up of the earlier developed spinodal network during the intermediate and late stages. This thought is supported by the rather uniform particle size distribution disclosed in the accompanying SEM image. The final result for the 25 wt% $PCL_{50,000}$ blend after curing at 180 °C is a phase inverted structure. Such a demixing behaviour is observed for this blend composition at all curing temperatures, for the 20 wt% $PCL_{50,000}$ blends cured at 200 and 180 °C as well as for all the 30 and 40 wt% PCL_{5000} blends. As mentioned earlier small PCL rich inclusions inside the epoxy particles are found in the SEM images, pointing at a secondary phase separation. These inclusions are too small to be seen by SALLS.

A phase-inverted structure is also obtained after curing a 30 wt% $PCL_{50,000}$ blend at the same temperature. The evolution of the SALLS patterns in Fig. 8(d), however, reveals that in this case no spinodal decomposition is involved. All particles are directly generated via nucleation and growth. This process is also relevant for the 40 and 50 wt% $PCL_{50,000}$ blends as well as for the 50 wt% PCL_{5000} blends.

The phase separation mechanisms observed at the onset of phase separation of both DDS-cured DGEBA/$PCL_{50,000}$ and DGEBA/PCL_{5000} blends with varying compositions and different curing temperatures are summarised in the Tables 5 and 6. The numbers between brackets represent the onset times of phase separation.

4. Discussion

Cheng and Chang first reported the LCST behaviour of DGEBA/DDS/PCL blends [29]. When polymerisation proceeds the molar mass of the epoxy resin increases by which the demixing region shifts to lower temperatures. When the demixing gab crosses the curing temperature, phase separation is induced. Inoue and co-workers [30] described this kind of behaviour for an epoxy/polyether sulphone (PES) blend. Clarke et al. published some theoretical considerations on this matter [31]. They treated the phase behaviour of blends consisting of a monodisperse linear polymer with a reacting network forming polymer. In this context the epoxy and hardener are modelled as a single component, by which the treatment simplifies from a three-component to a two-component system. This approach permits to calculate cloudpoint curves, spinodal lines and coexistence curves. The critical point is situated at the crossing point of the spinodal and cloudpoint curves. The most pertinent conclusions are summarised below as they permit to understand—at least

qualitatively—the results reported in the present paper. For details the reader is referred at the original publication.

(A) The critical concentration of the linear polymer shifts to lower values with increasing molar mass of the linear polymer but is not very sensitive to the increasing molar mass of the reacting network forming polymer ($\tau = 2.5$). The critical concentration of mixtures with a typical linear polymer occurs at concentrations far below 50% linear polymer.

(B) For systems that display LCST behaviour (negative b-coefficient [31]) the temperature at which samples with a critical composition demix (critical temperature) shifts to lower temperatures upon curing. Samples with concentrations close to the critical concentration demix via spinodal decomposition.

(C) At subcritical linear polymer concentrations (i.e. concentrations below the critical one) the spinodal and cloudpoint curves run upwards steeply with temperature and nearly coincide, resulting in a very narrow temperature range for demixing via nucleation and growth.

(D) At supercritical linear polymer concentrations (i.e. concentrations higher than the critical one) the cloudpoint curve readily extends to very high concentrations of linear polymer and shifts to lower temperatures faster than the spinodal line does with increasing degree of curing, resulting in a broad compositional and temperature range for demixing via nucleation and growth. However, when the curing reaction approaches the stage of gelation (molecules are formed of nominal infinite molar mass) the spinodal line rapidly catches up with the cloudpoint curve by which demixing is bound to occur via spinodal decomposition.

(E) When phases separate, a phase is created that essentially contains the high molar mass fraction of the reacting branched (epoxy) molecules. The phase rich in linear polymer contains the reacted low molar mass entities as well as the monomeric substances that did not yet react. As a result the curing reaction may well continue at the highest rate in the linear polymer rich phase.

(F) Right after phase separation, the cloudpoint curve associated with the composition (and temperature) of the linear polymer rich phase has shifted again to higher temperatures. However, the reaction goes on by which the molar mass of the branched epoxy molecules increases and the demixing region again crosses the curing temperature. Depending on the instantaneous composition of this earlier separated phase, demixing occurs via spinodal decomposition or nucleation and growth. When the primary phase separation occurred spinodally, it is very unlikely that also the newly formed phase (rich in linear polymer) has a composition that is sufficiently close to the critical concentration and accordingly, secondary phase separation usually occurs via nucleation and growth. On the other hand, when the reaction has proceeded close to gelation, spinodal decomposition is more likely.

(G) The epoxy rich phase that formed after primary phase separation is very poor in linear polymer and as such—as the reaction goes on—does not easily re-enter the demixing gab. Moreover, the low amount of non-reacted species in this phase considerably slows down the reaction here as compared to the linear polymer rich phase. If phase separation occurs again, this will be via a nucleation and growth process.

(H) In principle, during secondary phase separation again phases are formed in which the reaction may continue, potentially triggering a tertiary phase separation.

Critical concentrations in this study were assigned to compositions at which the phase-separated volumes occupy each 50% of the total volume. These are 25 wt% PCL_{5000} and 15 wt% $PCL_{50,000}$. The two mentioned samples are together with the 20 wt% $PCL_{50,000}$ blend cured at 150 °C the only ones in which the co-continuous structure is preserved. The fact that a phase occupancy of 50% coincides with the occurrence of a co-continuous morphology indicates that the viscosity of the phases is comparable, at least when demixing occurs.

As expected, the critical concentration shifts to lower PCL concentration with increasing PCL molar mass. Both phases after spinodal decomposition display a secondary phase separation involving the development of particles. Moreover, as broken epoxy beads (generated in the process of secondary phase separation) exhibit small spherical PCL-rich inclusions, tertiary phase separation occurs in these systems too!

The development of particles may point at phase separation by nucleation and growth, implying that the reaction did not yet reach the extent of gelation since in that case a secondary spinodal decomposition would have been observed. However, the appearance and growth of spherical particles is not necessarily a signature for demixing via nucleation and growth in the metastable region of a phase diagram when visco-elastic effects influence the phase separation. Deviating behavior is relevant for 'dynamically asymmetric' mixtures [27]. For sure mixtures of PCL with gelled or nearly gelled epoxy belong to this category, with the reacted epoxy fraction being the dynamically slow component. In this case co-continuous structures only appear in the unstable region of the phase diagram very close to the 'static symmetry line' [27]. At lower PCL content (but still in the unstable region) one may obtain sponge like structures involving small PCL rich droplets in an epoxy rich matrix and at the other side of the unstable region one may observe a so-called moving droplet phase of highly viscous epoxy rich particles in a PCL rich matrix. Such a phase separation can easily be confused with classical nucleation and growth phase separation as morphologically they can hardly be distinguished. However, the degree of epoxy conversion at phase separation (see below) strongly suggests the relevance of visco-elastic effects and casts doubt on the nucleation and growth hypothesis carried along in the result section. Phase separation within the unstable region that results in a sponge like structure may well be applicable to the blends with a low PCL concentration (5 and 10%) or to the secondary phase separation of PCL in the epoxy rich phase established during primary phase separation. Similarly, the droplets in the blends

with 50 wt% PCL_{5000} or with 30, 40 or 50 wt% $PCL_{50,000}$ could very well be associated with a 'moving droplet phase' rather than with a creation via nucleation and growth.

The supercritical blends 20 wt% $PCL_{50,000}$ (cured at 200 and 180 °C), 25 wt% $PCL_{50,000}$, 30 wt% PCL_{5000} and 40 wt% PCL_{5000} demix via spinodal decomposition and turn into a phase inverted structure by the break up into particles. Fractured epoxy beads reveal the occurrence of a secondary phase separation. Such a secondary separation may also have occurred inside the PCL rich phase but may remain undiscovered. Isolated epoxy rich droplets created during this secondary phase separation would for sure be washed out together with the PCL matrix in which they are imbedded. Alternatively, these secondary epoxy droplets may reach a size that is close to that of the primary ones by which they become indistinguishable in a SEM image. At an intermediate state of secondary growth a bimodal epoxy-rich particle size distribution would appear. In fact the image 5Bd suggests such a scenario.

The subcritical blends 15 and 20 wt% PCL_{5000} also demix in a spinodal way and break up to form particles. Here the particles are PCL rich. Again, it is hard to judge whether or not there is also a secondary phase separation. In any case the particle size histograms that result from the image analysis procedure are unimodal and can be well described by simple Gaussians. This also holds for the 5 and 10 wt% PCL_{5000} and $PCL_{50,000}$ blends that phase separate via the formation of particles.

The data in the Tables 5 and 6 demonstrate that temperature does not have a important effect on the phase separation mechanism and resulting phase morphology, at least not in the temperature range between 150 and 200 °C. The only items worth mentioning are that (1) phase separation is triggered earlier with increasing temperature due to the increased reaction rate, (2) the kinetics of phase separation are faster and (3) the particle sizes in particle-matrix structures but more importantly, the 'excess' volume associated with the particles increases a little with increasing cure temperature, pointing at an increasing degree of partial miscibility of the components at demixing. The T_g reaches the cure temperature earlier when curing is conducted at a higher temperature, at least for the samples for which a T_g could be determined. However, the morphologies become stable (i.e. the SALLS patterns no longer change) well before vitrification sets in. Most likely phase separation and coarsening is put to an end by gelation rather than vitrification. Unfortunately, gelation is hard to measure in situ [32].

Increasing the amount of PCL retards the curing reaction of the DGEBA/DDS mixture and therefore as a consequence the phase separation takes place at a later period and the time scale for primary demixing increases [13]. Phase separation in blends containing $PCL_{50,000}$ occurs earlier than in blends with PCL_{5000} and the difference becomes more pronounced at lower curing temperatures.

We also determined the degree of epoxy conversion as a function of time at the different curing temperatures by means of DSC [24]. If the degree of conversion at phase separation were plotted as a function of composition rather than the cure time, the data points of the different temperatures tend to collapse on a single, PCL molar mass dependent degree of conversion. All PCL_{5000} blends, independent of the curing temperature and hardly dependent of the blend composition, phase separate at an epoxy conversion close to 0.6 whereas the $PCL_{50,000}$ blends do so at a conversion of about 0.45. The value of 0.6 coincides with the degree of conversion at which the molar mass of the epoxy is expected to diverge, i.e. 0.58 [29,33]. $PCL_{50,000}$ demixes at a lower epoxy conversion due to the lower entropy of mixing. Note, however, that we do not want to claim that there is no temperature dependence associated with the demixing process. The degree of conversion at demixing cannot be determined very accurately and does not allow judging minor temperature dependencies. In any case it seems that the reaction rate and the associated epoxy molar mass built up is more sensitive to temperature than the mutual solubility, at least in the temperature and blend composition range studied here.

5. Conclusions

The reaction induced phase separation in blends of 4,4′-diaminodiphenyl sulphone (DDS) cured diglycidyl ether of bisphenol-A (DGEBA) with poly(ε-caprolactone) (PCL) behaves qualitatively as can be expected from earlier theoretical work. Prior to curing the blends are fully miscible. An LCST demixing region develops upon curing, which shifts to lower temperatures while the reaction is progressing. When the demixing region crosses the curing temperature liquid–liquid phase separation is induced. The mechanism depends essentially on the blend composition. At a given PCL molar mass and curing temperature compositions that are close to the critical concentration demix via spinodal decomposition. However, the associated, typical co-continuous morphology is only preserved for the actual critical compositions. The initial co-continuous structure for off-critical compositions rapidly breaks up into spherical particles, which for subcritical and supercritical initial PCL concentrations are PCL and epoxy-rich respectively. The curing reaction proceeds after the primary phase separation and induces a secondary phase separation. This occurs in both phases for the critical compositions, but is only clearly revealed in the epoxy droplets for blends with initial supercritical PCL concentrations. Moreover, also the epoxy rich droplets in blends with a critical concentration that are generated in the secondary phase separation process, reveal PCL rich sub-inclusions due to a tertiary phase separation process. Off critical compositions that are further away on either side from the critical point phase separate via the direct formation of spherical particle most likely as a result of the dynamic asymmetry of these blends.

An increase of the PCL molar mass makes the critical composition shift to a lower PCL concentration and shifts forward the time of demixing. The reacting species are diluted progressively with increasing PCL mass fraction by which the reaction rate is reduced and the time for demixing is postponed. Increasing the curing temperature induces a faster reaction and enhances phase separation. The final morphology, however,

does not strongly depend on the curing temperature. Vitrification occurs well after the morphology has stabilised, indicating that gelation rather than vitrification stops the morphology development.

Acknowledgements

B. Goderis is a postdoctoral fellow of the Fund for Scientific Research Flanders (FWO-Vlaanderen). S. Goossens is indebted to the IWT for a research grant.

References

[1] Riew CK, Gilham JK, editors. Rubber-modified thermoset resins. Washington, DC: American Chemical Society; 1984 [Adv. Chem. Ser. No. 208].
[2] Riew CK, editor. Rubber-toughened plastics. Washington, DC: American Chemical Society; 1989 [Adv. Chem. Ser. No. 222].
[3] Riew CK, Kinloch AJ, editors. Toughened plastics. Part I. Science and engineering. Washington, DC: American Chemical Society; 1993 [Adv. Chem. Ser. No. 223].
[4] Bucknall CB, editor. Toughened plastics. London: Applied Science Publisher; 1977.
[5] Dusek K, Pascault JP. The Wiley polymer networks group review series. New York: Wiley; 1998 p. 277.
[6] Girard-Reydet E, Rinardi CC, Sautereau H, Pascault JP. Macromolecules 1995;28:7608.
[7] Bauer RS, editor. Epoxy resin chemistry. Washington, DC: American Chemical Society; 1979 [Adv. Chem. Ser. 114].
[8] Pascault JP, Williams RJJ. Formulation and characterization of thermoset–thermoplastic blends. In: Paul DR, Bucknall CB, editors. Polymer blends. Formulation, Vol. 1. New York: Wiley; 2000. p. 379–415.
[9] Kim BS, Chiba T, Inoue T. Polymer 1993;34:2809.
[10] Girard-Reydet E, Sautererau H, Pascault JP, Keates P, Navard P, Thollet G, et al. Polymer 1998;39:2269.
[11] Ishii Y, Ryan AJ. Macromolecules 2000;33:158.
[12] Kim BS, Chiba T, Inoue T. Polymer 1995;36:67.
[13] Yamanaka K, Inoue T. Polymer 1989;30:662.
[14] Eliçabe GE, Larrondo HA, Williams RJJ. Macromolecules 1998;31:8173.
[15] Hoppe CE, Galante MJ, Oyanguren PA, Williams RJJ. Macromolecules 2002;35:6324.
[16] Gan W, Yu Y, Wang M, Tao Q, Li S. Macromolecules 2003;36:7746.
[17] Swier S, Van Mele B. Polymer 2003;44:2689.
[18] Ishii Y, Ryan AJ, Clarke N. Polymer 2003;44:3641.
[19] Swier S, Van Mele B. Polymer 2003;44:6789.
[20] Guo Q, Harrats C, Groeninckx G, Koch MHJ. Polymer 2001;42:4127.
[21] Guo Q, Harrats C, Groeninckx G, Reynaers H, Koch MHJ. Polymer 2001;42:6031.
[22] Guo Q, Groeninckx G. Polymer 2001;42:8647.
[23] Guo Q. Thermosetting polymer blends: miscibility, crystallization and related properties. In: Shonaike GO, Simons G, editors. Polymer blends and alloys New York: Marcel Dekkers; 1999, chapter 6.
[24] Vanden Poel G. PhD Thesis, KuLeuven, Belgium; 2003 [chapter 2].
[25] Gordon M, Taylor JS. J Appl Chem 1952;2:495.
[26] Koningsveld R, Stockmayer WH, Nies E. Polymer phase diagrams, a textbook. New York:Oxford University Press; 2001.
[27] Tanaka H. J Phys: Condens Matter 2000;12:R207–R64.
[28] Olabisi O, Robeson LM, Shaw MT. Polymer–polymer miscibility. New York: Academic Press; 1979.
[29] Chen JI, Chang FC. Polymer 2001;42:2193.
[30] Ohnaga T, Chen W, Inoue T. Polymer 1994;35:17.
[31] Clarke N, McLeish TCB, Jenkins SD. Macromolecules 1995;28:4650–9.
[32] Bonnet A, Pascault JP, Sautereau H, Camberlin Y. Macromolecules 1999;25:286.
[33] Hofmann K, Glasser WG. Thermochim Acta 1990;166:169.